Multiple-resonance local wave functions for accurate excited states in quantum Monte Carlo

Habiburrahman Zulfikri,[1] Claudio Amovilli,[2] and Claudia Filippi[1,*]

[1]*MESA+ Institute for Nanotechnology, University of Twente, P.O. Box 217, 7500 AE Enschede, The Netherlands*
[2]*Dipartimento di Chimica e Chimica Industriale, Università di Pisa, Via Giuseppe Moruzzi 13, 56124 Pisa, Italy*

We introduce a novel class of local multideterminant Jastrow-Slater wave functions for the efficient and accurate treatment of excited states in quantum Monte Carlo. The wave function is expanded as a linear combination of excitations built from multiple sets of localized orbitals that correspond to the bonding patterns of the different Lewis resonance structures of the molecule. We capitalize on the concept of orbital domains of local coupled-cluster methods, which is here applied to the active space, to select the orbitals to correlate and construct the important transitions. The excitations are further grouped into classes, which are ordered in importance and can be systematically included in the Jastrow-Slater wave function to ensure a balanced description of all states of interest. We assess the performance of the proposed wave function in the calculation of vertical excitation energies and excited-state geometry optimization of retinal models whose $\pi \rightarrow \pi^*$ state has a strong intra-molecular charge-transfer character. We find that our multi-resonance wave functions recover the reference values of the total energies of the ground and excited states with only a small number of excitations and that the same expansion can be flexibly used at very different geometries. Furthermore, significant computational saving can also be gained in the orbital optimization step by selectively mixing occupied and virtual orbitals based on spatial considerations without loss of accuracy on the excitation energy. Our multi-resonance wave functions are therefore compact, accurate and very promising for the calculation of multiple excited states of different character in large molecules.

I. INTRODUCTION

The development of local correlation methods to describe multiple electronic states of extended molecular systems is a very active and exciting research area in computational chemistry. By expressing the wave function in a local orbital basis, one can make use of the assumption that electron correlation is a local phenomenon for instance for nonmetallic systems in the ground state [1]. In so doing, a local occupied orbital or an orbital pair only correlates to a subset of local virtual orbitals selected on the basis of certain criteria such as spatial considerations [2, 3], the threshold on the magnitude of the exchange integrals [4], or the threshold on the occupation number of virtual pair natural orbitals [5, 6]. A local approach has clear advantages over traditional methods using delocalized orbitals, where all occupied orbitals correlate to the virtual ones. For the ground state, the local scheme has been implemented in several single-reference methods such as the configuration-interaction [7–9], coupled-cluster [2, 3, 6, 10, 11], and perturbation [12–15] approaches as well as in various multi-reference methods [4, 16–21]. The extension of the local ansatz to excited states is however not straightforward since the excited state may be characterized by non-local transitions and, importantly, multiple states have to be treated at the same level of accuracy [16, 22–27].

Quantum Monte Carlo (QMC) methods which provide a stochastic approach to the solution of the many-body problem, can also benefit from the use of local orbitals. In the commonly employed Jastrow-Slater wave functions, the Jastrow factor recovers dynamic correlation whereas static correlation is addressed through a symmetry-adapted linear combination of Slater determinants which can be built out of local or delocalized orbitals. To construct the determinantal component, a set of relevant orbitals is selected and often correlated in a (nearly) complete active space (CAS) expansion to capture the desired chemical features in the application of interest. Unfortunately, the dimension of such an expansion grows dramatically (exponentially in the CAS case) with the system size and hence hinders its application to large molecules. As the system grows, truncation of the expansion is therefore inevitable and a simple procedure as the use of a threshold on the coefficients does not guarantee the same expansion size at different geometries. Consequently, it becomes difficult to maintain an affordable number of determinants and ensure a balanced description of different parts of the potential energy surface of all the states under consideration.

The availability of accurate Jastrow-Slater wave functions with a small and transferable determinantal component is therefore highly desirable. In the previous work with Fracchia, we have shown that this is possible with the use of orbitals localized over one or two centers and introduced a local correlation scheme in QMC to progressively construct accurate and compact multi-determinant wave functions of increasing quality, which were successfully applied to the ground state of closed and open shell systems [28–30]. By correlating two pairs of electrons sitting in adjacent bonding orbitals with the corresponding anti-bonding orbitals, we achieved linear scaling and, consequently, a significant computational gain with respect to other local expansions also employed in QMC as in the perfect-pair generalized-valence-bond [31] or the valence-bond approach built on atomic-centered orbitals [32].

In general, our ground-state scheme breaks down for excited states since transitions between orbitals separated by several bonds may acquire significant weight in the many-body wave function if the excited state has charge-transfer or Rydberg character. The first important step is therefore to understand how to select which orbitals we want to correlate to account for the most important determinants in the

* c.filippi@utwente.nl

ground and/or the excited states. To this aim, we capitalize on the concept of orbital domains of local coupled-cluster methods [2, 3, 22–24] which we apply here to the local orbitals in the active space. We further classify the excitations in classes and include them progressively into the expansion of the Jastrow-Slater wave functions so that multiple states of different character are treated on an equal footing. Such a procedure allows us to control what enters in our wave functions but the key step to ensure a compact and transferable determinantal expansion is to also account for the multiple Lewis resonance structures of the molecule, whose relative importance may change in different structural configurations or electronic states. We therefore construct the domains and excitation classes for all sets of local orbitals corresponding to the multiple resonance structures and write the wave function as a linear combination of the resulting determinants. We demonstrate the excellent performance of our compact multi-resonance local Jastrow-Slater wave functions in the calculation of the vertical excitation and geometry optimization of the charge-transfer $\pi \rightarrow \pi^*$ state of retinal model chromophores.

The subsequent part of the paper is organized as follow. In section II, we illustrate the concept of orbital domains and excitation classes for multiple resonance structures. The computational details are presented in section III and the performance of our method is demonstrated in section IV. We conclude in section V.

II. METHOD

To illustrate the potential of a local approach in QMC, we briefly describe the linear-scaling scheme we recently introduced for ground states, which couples electron pairs locally to progressively construct wave functions of increasing quality [28–30]. In our approach, the occupied orbitals in the reference are localized over one or two centers along with the corresponding antibonding orbitals in the virtual space. The determinants are then generated by correlating two pairs of electrons sitting in adjacent bonding orbitals and the corresponding two antibonding orbitals in a so-called CAS(4,4) expansion (i.e. by including the excitations in the active space obtained by correlating four electrons in the two bonding and two antibonding orbitals). Importantly, we demonstrated in our previous work that it is possible to classify the resulting transitions in classes of increasing importance and, in so doing, building a set of modular wave functions of growing complexity. Since electrons located in separated orbitals are not correlated, the number of determinants in the wave function scales linearly with the size of the molecule.

To understand the difficulties of extending our local scheme to excited states and how we will solve them, we consider the retinal protonated Schiff base chromophore with three conjugated π bonds (PSB3) of Figure 1, which, despite its apparent simplicity, represents a challenging model for the study of retinal photochemistry. This molecule well exemplifies the complications occurring in the excited state since its $\pi \rightarrow \pi^*$ excitation is accompanied by significant transfer of electronic charge from the carbon to the nitrogen terminus (or, equivalently, of positive charge in the opposite direction).

To account in a balanced manner for static correlation in the ground and excited states, one could adopt a delocalized description in terms of three delocalized π bonding and three π^* antibonding orbitals (panel A) and correlate the six electrons in the resulting active space, constructing a minimal CAS(6,6) expansion. In addition to this standard representation of the determinantal component of the wave function, we can however construct by unitary transformation not one but three equivalent sets of localized π orbitals, corresponding to the three possible Lewis resonance structures. These different local orbital pictures will be more suitable to describe the electronic structure of PSB3 at different geometries or in different states: While the first resonance structure (Res-1) is dominant at the ground-state equilibrium, we anticipate that the other resonance structures will be very important in the treatment of the $\pi \rightarrow \pi^*$ excitation with its strong charge-transfer character. In general, all resonance structures will be visited in different regions of the excited-state potential energy surface. We stress that, if we include all excitations in the active space, these orbital representations are equivalent and one will recover the same amount of electronic correlation. The goal here is however to find a representation and a set of rules which result in a compact wave function without including all excitations, given their exponentially growing number with system size.

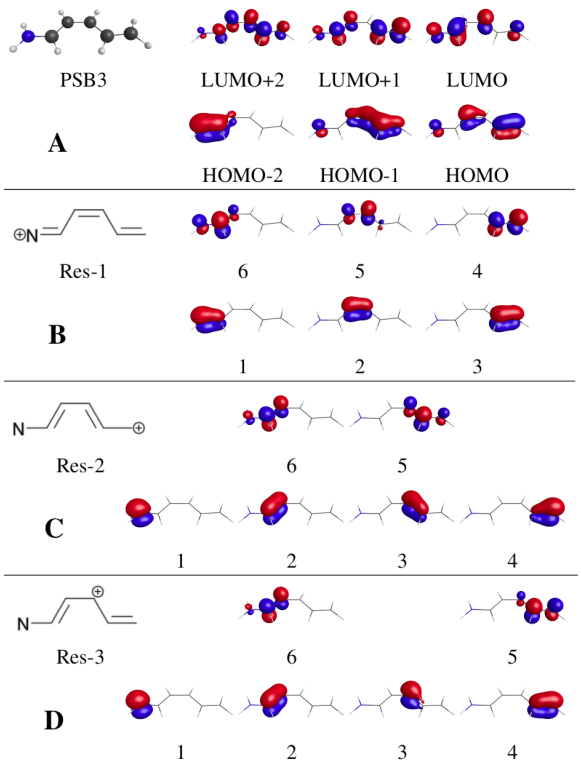

FIG. 1. PSB3: (A) Active delocalized π orbitals obtained at the CASSCF(6,6) level, and (B-D) three unitary transformed sets of localized orbitals corresponding to the three Lewis resonance structures.

It is rather straightforward to understand the failure of our ground-state local correlation scheme if we focus on the dominant Lewis structure at equilibrium (panel B) and on a multi-determinant expansion on the corresponding local orbitals. As discussed below, an analysis of the dominant single-electron transitions reveals that spatially remote orbitals are coupled (e.g. bonding orbital 3 with antibonding orbital 6). Consequently, we cannot adopt the set of rules described above for ground states since it is impossible to simply correlate adjacent pairs of bonding/antibonding orbitals.

A. Domains and excitation classes

To select the orbitals to correlate, we borrow the concept of *orbital domains* from local-correlation methods [1–3, 7, 22–24] and adapt it to the advantageous features of quantum Monte Carlo. Here, we define a domain as an orbital in the reference and the set of orbitals which are coupled to it by a large single-electron transition in the multi-determinant wave functions of the states of interest. As threshold on the weight to select the important singles, we choose to use the highest weight in any of the states under consideration so that all orbitals in the active space appear at least in one single excitation. In building our multi-determinant wave functions, we will then only retain the domains characterized by large single transitions and generate the double and higher excitations within and from the union of the surviving domains. Differently from conventional local schemes in quantum chemistry, we will construct the domains only from the orbitals within the active space (letting the Jastrow factor and, subsequently, diffusion Monte Carlo recover dynamical correlation) and also attempt to further classify the resulting excitations to generate a set of wave functions of increasing complexity as we had done for ground states.

To illustrate our scheme and investigate whether it can lead to a balanced description of the ground and excited states, we first focus on PSB3 at equilibrium and the Res-1 local orbital representation (Figure 1), and compute the CASSCF wave functions correlating the three bonding orbitals (labeled 1,2,3) and three antibonding orbitals (labeled 4,5,6) in a CAS(6,6) expansion. Through the analysis of weights of the configurations state functions entering the wave function, we can identify whether the subset of configurations generated with the use of orbital domains recovers most of the weights of the wave functions in both states and which excitation classes may potentially be neglected when using such determinantal component in a QMC calculation.

If one defines a reference configuration as a configuration in the ground state consisting of doubly-occupied localized bonding orbitals, there is only one such configuration for the Res-1 representation of PSB3, namely 222000, where a configuration is denoted as $\mathrm{n}_1\mathrm{n}_2\mathrm{n}_3\mathrm{n}_4\mathrm{n}_5\mathrm{n}_6$ with n_m the occupation number of orbital m. To build the domains, we now consider the single excitations out of the reference in the Res-1 wave function of the $\pi \rightarrow \pi^*$ state and find that, as reported in Table I, there are several single-electron transitions carrying significant weight, differently to what one would obtain in an expansion over delocalized orbitals where the HOMO-LUMO transition is instead dominant. Due to the charge-transfer nature of the excited state, the single excitations connect the bonding to the antibonding orbitals sitting on their left and grouping the orbitals in two separate CAS(4,4) active spaces over pairs of adjacent bonding/antibonding orbitals (i.e. 1,2,5,6 and 2,3,4,5) as in our ground-state scheme would miss the second most important single excitation in a CAS(6,6) expansion, namely, the $3 \rightarrow 6$ transition. Furthermore, a similar analysis of the wave function for larger models of the retinal chromophore (with one, two, and three additional double bonds, namely, PSB4, PSB5, and PSB6) indicate that this behavior will persist and that far away orbitals will remain correlated even though to a lesser extent (see Tables S16, S28, and S29). This is clear evidence that, for this problem, a large active space cannot be divided into several smaller active spaces on the basis of spatial vicinity of the orbitals but a different procedure must be followed to construct our wave function.

If we select the singles to build the domains so that all active orbitals are involved in at least one transition, we find that there are 6 important singles out of the reference (corresponding to a maximum weight of 2.19% in the excited state) and, correspondingly, three domains:

a) $\{1:6\}$
b) $\{2:5,6\}$
c) $\{3:4,5,6\}$

For each domain, the number before the colon represents the doubly-occupied orbital in the reference which is linked via a single excitation to an empty orbital appearing after the colon. As already mentioned, the purpose of establishing the domains is to construct doubles and higher excitations by coupling the domains and to achieve in this way a compact form of the wave function. Therefore, while all domains can in principle be employed in generating higher transitions, we note that the most important singles belong to the **b** and **c** domains and choose to neglect the least important **a** domain, only retaining the singles within this domain and selected transitions as explained below.

We collect the configurations considered so far in the three excitation classes denoted as X0, X1, and X2, comprising the reference, the singles belonging to the dominant domains, and the important singles of the remaining domains, respectively. As next excitation class (X3), we include in our wave functions all double excitations from a bonding to its corresponding antibonding orbital, namely, $(1 \rightleftarrows 6)$, $(2 \rightleftarrows 5)$, and $(3 \rightleftarrows 4)$. The importance of these excitations for the ground state was highlighted in our work on the development of a local correlation scheme for ground states [28] and is here corroborated in the PSB3 system: With the inclusion of the X3 class, the configurations make up 97.56% of the total ground-state CASSCF wave function. On the other hand, the X0-X3 classes only account for 89.67% of the total weight in the excited state.

To further improve the quality of the wave functions (in this case, the excited-state one), we need to include additional

TABLE I. PSB3: CASSCF weight percentage of configurations with localized Res-1 orbitals computed at the S0 B3LYP equilibrium geometry.

	Type	Domain	CSF	Det	Configuration	Weight (%)	
			(N)	(N)	(1,2,3,4,5,6)	S0	S1
X0	ref		**1**	**1**	222000	**89.50**	**0.16**
X1	S	**b**	1	2	212010	0.01	13.43
	S	**b**	1	2	212001	0.46	18.6
	S	**c**	1	2	221100	0.02	3.05
	S	**c**	1	2	221010	0.24	27.26
	S	**c**	1	2	221001	0.26	21.03
Sub			**5**	**10**		**0.99**	**83.37**
X2	S	**a**	**1**	**2**	122001	**0.00**	**2.19**
X3	D	**a**	1	1	022002	1.11	0.76
	D	**b**	1	1	202020	2.31	2.75
	D	**c**	1	1	220200	3.65	0.44
Sub			**3**	**3**		**7.07**	**3.95**
X4	D	**b**	1	1	202002	0.27	0.83
	D	**c**	1	1	220020	0.10	0.62
Sub			**2**	**2**		**0.37**	**1.45**
X5	D	**b+c**	2	6	211110	0.45	0.08
	D	**b+c**	2	6	211101	0.03	0.73
	D	**b+c**	2	6	211011	0.08	1.39
Sub			**6**	**18**		**0.56**	**2.20**
X6	D	**b+c**	1	2	211020	0.01	0.57
	D	**b+c**	1	2	211002	0.05	0.51
Sub			**2**	**4**		**0.06**	**1.08**
X7	D	**b**	1	2	202011	0.01	0.04
	D	**c**	1	2	220110	0.21	0.24
	D	**c**	1	2	220101	0.02	0.26
	D	**c**	1	2	220011	0.01	0.32
Sub			**4**	**8**		**0.25**	**0.86**
X8	T	**b**+X3	1	2	210210	0.00	0.34
	T	**b**+X3	1	2	210201	0.01	0.46
	T	**b**+X3	1	2	012012	0.00	0.08
	T	**c**+X3	1	2	201021	0.00	0.53
	T	**c**+X3	1	2	201120	0.00	0.01
	T	**c**+X3	1	2	021012	0.00	0.11
	T	**c**+X3	1	2	021102	0.00	0.03
Sub			**7**	**14**		**0.01**	**1.56**
Total			**31**	**62**		**98.92**	**98.03**

double configurations, which we generate by coupling the single excitations within and between the dominant **b** and **c** domains. The transitions are then classified based on the orbital occupations and the resulting new excitation classes ordered according to their importance in the multi-determinant expansion. For instance, by coupling the single excitations within the **c** domain $\{3:4,5,6\}$, we obtain

$$220200 = (3 \rightrightarrows 4)$$
$$220020 = (3 \rightrightarrows 5)$$
$$220002 = (3 \rightrightarrows 6)$$
$$220110 = (3 \to 4) + (3 \to 5)$$
$$220101 = (3 \to 4) + (3 \to 6)$$
$$220011 = (3 \to 5) + (3 \to 6)$$

where $(3 \rightrightarrows 4)$ was already considered as a member of the X3 class. Configurations which are double excitations from a bonding to an adjacent antibonding orbitals are classified as X4 excitations, where orbitals are deemed adjacent only if located close to each other and not separated by an atom. Doubles from a bonding to a separated antibonding orbital, e.g. $(3 \rightrightarrows 6)$, are found to have negligible weight and are therefore not included in the X4 class. Double excitations from one bonding to two different antibonding orbitals form the X7 excitation class.

From the coupling of single excitations between the two **b** and **c** domains, we obtain the following doubles

$$211110 = (2 \to 5) + (3 \to 4)$$
$$211020 = (2 \to 5) + (3 \to 5)$$
$$211011 = (2 \to 5) + (3 \to 6)$$
$$211101 = (2 \to 6) + (3 \to 4)$$
$$211002 = (2 \to 6) + (3 \to 6)$$

Doubles with 4 unpaired electrons are classified as X5 and doubles from two bonding orbitals to the same antibonding orbital are denoted as X6, which exhausts the possible doubles one can build within one or two domains. We note that the ordering in importance of the X4-X7 doubles can be different for other states or molecules but, in this work, we will use the aforementioned ordering. The next excitation class (X8) is given by the triples constructed as the double excitations from a bonding to its corresponding antibonding orbital combined with singles from the X1 class.

One can of course continue to construct further excitation classes and also couple more than two domains until all configurations in the CAS(6,6) active space are included. Here, we however stop at X8 since the X0–X8 excitation classes cover ∼98% of the weight of both S0 and S1 states at the equilibrium geometry. The state-averaged CASSCF weights of all configurations in the excitation class of PSB3 with the Res-1 orbitals are listed in Table I and the description of excitation classes is summarized in Table II.

TABLE II. Description of excitation classes. The X4-X7 excitations are built from the domains.

Class	Description
X0	References (all doubly-occupied bonding)
X1	Important singles in dominant domains to build the doubles
X2	Important singles in other domains
X3	Bonding-antibonding doubles
X4	Doubles to adjacent antibonding
X5	Doubles (4 unpaired electrons)
X6	Doubles (2 unpaired electron in bonding orbitals)
X7	Doubles (2 unpaired electron in empty orbitals)
X8	Triples (bonding-antibonding doubles plus X1 singles)

So far, our analysis demonstrates that the concept of orbital domains as identified at the CASSCF level leads to the construction of some of the most important excitation classes for both states. One may however ask whether these configurations remain important once we optimize the orbitals in the presence the Jastrow factor in a so-called Jastrow-Slater wave function:

$$\Psi = \mathcal{J} \sum_{i}^{N_{\text{CSF}}} c_i \, C_i \, ,$$

where C_i are the configuration state functions (CSF) and $\mathcal{J}$ is the Jastrow correlation function explicitly depending on the inter-electronic coordinates. In optimizing the orbitals, we do not preserve orthogonality among them, so the square of a CI coefficient in a Jastrow-Slater wave function is not the weight of a configuration. Therefore, we use the following definition of the weight of configurations in terms of the overlap $S_{ij} = \langle \mathcal{J}C_i | \mathcal{J}C_j \rangle$:

$$w_i = \frac{1}{q_{\text{norm}}} \left(c_i S_{ii} c_i + \sum_{j \neq i}^{N_{\text{CSF}}} c_i S_{ij} c_j z_{ij} \right) , \qquad (1)$$

where the norm of the wave function is given by

$$q_{\text{norm}} = \sum_{i}^{N_{\text{CSF}}} \sum_{j}^{N_{\text{CSF}}} c_i S_{ij} c_j \, , \qquad (2)$$

and, to reduce the occurrence of unphysical negative weights, we introduced the damping factor

$$z_{ij} = \frac{2(c_i S_{ii})^2}{(c_i S_{ii})^2 + (c_j S_{jj})^2} \, . \qquad (3)$$

As shown in Table III, the **variational Monte Carlo** (VMC) weights in a determinantal expansion over the Res-1 orbitals of PSB3 display a very good correspondence with the CASSCF weights. This ensures that the analysis of the excitation classes we have done above based on the CASSCF weights is transferable to VMC for this system.

TABLE III. PSB3: CASSCF and VMC weight percentage of the X0-X3 configurations of the first Res-1 structure computed at the S0 B3LYP equilibrium geometry. The VMC wave function includes all singles, doubles, and triples on the Res-1 local orbitals.

Class	Configuration	CASSCF (%)		VMC (%)	
	(1,2,3,4,5,6)	S0	S1	S0	S1
X0	222000	89.50	0.16	92.85	2.41
X1	221100	0.02	3.05	0.01	3.97
	221010	0.24	27.26	0.97	33.06
	221001	0.26	21.03	0.91	20.48
	212010	0.01	13.43	0.10	12.77
	212001	0.46	18.6	1.62	17.96
X2	122001	0.00	2.19	0.00	1.15
X3	220200	3.65	0.44	1.25	0.35
	202020	2.31	2.75	0.66	1.71
	022002	1.11	0.76	0.33	0.34

B. Beyond one resonance structure

The importance of each resonance structure representation is directly related to the internuclear distances of the molecular structure under study. Therefore, while all orbital representations of Figure 1 are equivalent if we retain the complete expansion, we can no longer rely on the use of a single resonance structure once the localized CAS expansion is truncated based on excitation classes. For the PSB3 example, this means that, if one adopts the Res-1 picture above at a different geometry, there is no guarantee that the resulting excitations sum up to a similar, balanced weight percentage of the total wave functions as in Table I. For instance, at a bond-inverted geometry which is more naturally described in terms of the Res-2 orbitals, the expansions constructed from the X0–X8 excitation classes over CASSCF orbitals of the Res-1 type only recover ∼98% and ∼74% of the total weights of the ground- and excited-state CASSCF wave functions, respectively (see Table S6).

In general, one might expect that all three resonance structures will be "visited" in different regions of the excited state potential energy surface of a molecule and that, to strive a balanced description of such diverse regions and account for changes in the relative importance of the three forms, our wave function should include all three of them. We can achieve this by taking advantage of the flexibility of the QMC method which allows us to work with an over-complete orbital set and write the Jastrow-Slater wave function as a linear combination of multiple Lewis structures, each expressed on a small set of determinants constructed according to the concepts of domains and excitation classes. Therefore, we rewrite the wave function in terms of all possible resonance structures of a molecule as

$$\Psi = \mathcal{J} \left(\sum_{i} c_i \, C_i^{\text{Res-1}} + \sum_{j} c_j C_j^{\text{Res-2}} + \cdots \right) , \qquad (4)$$

where $C_i^{\text{Res}-\text{I}}$ are the CSFs of the I-th resonance structure.

In constructing this multi-resonance wave function, it is desirable to adopt the same recipe for all resonance structures in the definition of the domains and the subsequent construction of the excitation classes. In the example of PSB3, the extension of the concept of orbital domains developed in the context of the Res-1 structure to Res-2 and Res-3 presents however a complication: In these two structures, the six π electrons see four bonding (labeled 1, 2, 3, 4) and two antibonding (labeled 5, 6) orbitals (see panels C and D in Figure 1). Therefore, bonding orbitals are not necessarily doubly-occupied in the reference and this imbalance is reflected in the absence of a dominant reference configuration. We can nevertheless proceed as before if we consider each reference in turn, and define a corresponding set of domains from which to construct the doubles and other excitations. The union of the resulting excitations will then form our multi-resonance wave function. To analyze whether this way of extending the concept of domains to Res-2 and Res-3 is successful in recovering a high

percentage of the total weights of the CASSCF wave functions, it is more appropriate to use a geometry where its internuclear distances resemble the bonding-antibonding structure of the resonance under study.

For the Res-2 structure, we therefore investigate the excitation classes using an in-plane bond-inverted geometry where we expect a description in terms of the Res-2 orbital set to be more suitable. By placing 6 electrons in 4 bonding orbitals, we can construct 4 doubly-occupied reference configurations: The important references are 222000, 220200, and 202200 and are included in the X0 class, while 022200 can be neglected since its weight is 0% in both states. From each reference, we then search for all important single excitations to build the domains. Here, a single excitation from a particular reference is a one-electron transition from a doubly-occupied bonding orbital to an empty (bonding or antibonding) orbital. Furthermore, one such transition may be obtained starting from more than one reference and therefore appear more than once as belonging to domains of different references. As in the case of Res-1, to decide which singles are important, we apply as threshold the maximum weight in either state so that all orbitals in the active space are involved in a single excitation (which is here 0.72% in the ground state). This criterion results in 9 important singles and three sets for domains as listed in Table IV. Using the same notation as for Res-1, the domains of the 222000 reference are :

1a) $\{1:4\}$
1b) $\{2:4\}$
1c) $\{3:4\}$

The domains of 220200 are

2a) $\{1:3\}$
2b) $\{2:3,5\}$
2c) $\{4:3\}$

and, for the 202200 reference, we have

3a) $\{1:2\}$
3b) $\{3:2,6\}$
3c) $\{4:2,6\}$

These singles are included in the X1 class except for the least important ($2 \rightarrow 5$) excitation of domain **2b**, which is included in the X2 class but further neglected in constructing the doubles to avoid many determinants with negligible weight on both states. Subsequent excitation classes are built and ordered according to the classification in the Res-1 structure as outlined in Table IV.

An analysis of the weights reveals that, also for this resonance structure, constructing the excitations based on the orbital domains and including the X0-X8 classes lead to a balanced description of the ground- and excited-state wave functions, recovering a substantial percentage of the total weight at the CASSCF level as shown in Table V. A complete list of the configurations built from the Res-2 orbitals is reported in Table S7. For the the construction of the domains and the weight analysis of the excitation classes of the third resonance structure (Res-3), we refer the reader to the Supporting Information (Table S9). The analysis is quite similar to the one of the Res-2 structure, since Res-3 is characterized by the same numbers of bonding and antibonding orbitals, and performed at a geometry constructed to have a bond-length pattern and CASSCF gap in between the values of the ground-state equilibrium and bond-inverted geometries. Importantly, the weights of the X0-X8 classes recover a very similar percentage of the ground- and excited-state CASSCF wave functions as in the case of the Res-2 structure.

Therefore, the set of rules we have developed based on the concept of domains satisfy the prerequisite to be applicable without adjustments to the rather different resonance structures of PSB3. In practice, the analysis of the resonance structures at the different geometries is only performed to establish the domains for the different resonances and construct the dominant configurations. Then, for the geometry of interest,

TABLE IV. PSB3: Construction of the excitation classes of the Res-2 structure. Excitations in square brackets correspond to configurations already obtained.

Class	Reference		
	222000	220200	202200
X1	$1 \rightarrow 4$	$1 \rightarrow 3$	$1 \rightarrow 2$
	$2 \rightarrow 4$	$2 \rightarrow 3$	$3 \rightarrow$ [2],6
	$3 \rightarrow 4$	$[4 \rightarrow 3]$	$4 \rightarrow$ [2],6
X2	-	$2 \rightarrow 5$	-
X3	$3 \rightrightarrows 5$	$2 \rightrightarrows 6$	$3 \rightrightarrows 5$
	$2 \rightrightarrows 6$		
X4	-	-	$[3 \rightrightarrows 6]$
X5	-	-	$1 \rightarrow 2+3 \rightarrow 6$
			$1 \rightarrow 2+4 \rightarrow 6$
			$3 \rightarrow 2+4 \rightarrow 6$
X6	-	-	$3 \rightarrow 6+4 \rightarrow 6$
X8	$1 \rightarrow 4+3 \rightrightarrows 5$	$1 \rightarrow 3+2 \rightrightarrows 6$	$1 \rightarrow 2+3 \rightrightarrows 5$
	$1 \rightarrow 4+2 \rightrightarrows 6$	$[4 \rightarrow 3+2 \rightrightarrows 6]$	$[4 \rightarrow 2+3 \rightrightarrows 5]$
	$2 \rightarrow 4+3 \rightrightarrows 5$		$4 \rightarrow 6+3 \rightrightarrows 5$
	$[3 \rightarrow 4+2 \rightrightarrows 6]$		

TABLE V. PSB3: CASSCF weight percentage of the excitation classes of the Res-2 structure. The in-plane bond-inverted S1 CASSCF geometry is used.

	CSF	Det	Weight (%)	
	(N)	(N)	S0	S1
X0	3	3	12.60	23.29
X1	8	16	76.92	64.64
X2	1	2	0.72	0.43
X3	4	4	0.42	0.94
X5	6	18	2.66	2.84
X6	1	2	0.33	1.07
X8	6	12	0.66	1.43
Total	**29**	**57**	**93.59**	**94.21**

different sets of equivalent local orbitals are generated and the CSFs we have identified as important are used in a Jastrow-Slater wave function. Below, using PSB3 and other retinal models, we will employ one- and multi-resonance Jastrow-Slater wave functions to assess the performance of the approach, namely, to investigate numerically which excitation classes mainly impact the quality of a calculation, the accuracy of a one- and multiple-resonance wave function with respect to the use of truncated expansion over delocalized orbitals, and the transferability of this framework to geometries characteristic of different parts of the excited-state potential energy surface.

C. Orbital Optimization

In the optimization of the orbitals of a monodeterminant Jastrow-Slater wave function, one mixes the occupied orbitals with the virtual ones of the same symmetry. In the multideterminantal case, the inactive orbitals are mixed with the active and virtual ones, and the active orbitals with other active and the virtual orbitals, always according to the symmetry. For large systems, the number of orbital mixing grows rapidly and, to maintain a low computational cost, one is often forced to select a subset of virtual orbitals to mix with the occupied ones: The delocalized virtual orbitals are for instance ordered energetically and the highest-energy virtual orbitals are omitted.

If we unitarily transform all (inactive, active, and virtual) delocalized orbitals into localized ones, we can employ a different criterion and selectively mix the orbitals based on spatial considerations. First, to establish the centers where an orbital is mainly localized, we use its expansion over the N_{bas} atomic basis functions χ_i as $\sum_i b_i \chi_i$ and evaluate the quantities ρ_a for all nuclei:

$$\rho_a = 2 \sum_{i}^{M_a} \sum_{j}^{N_{\text{bas}}} b_i^* b_j \langle \chi_i | \chi_j \rangle \,, \tag{5}$$

where the first summation only runs over the M_a atomic basis functions of nucleus a. A large value of ρ_a indicates that the orbital is mainly localized on atom a and one can use a threshold on the value of ρ_a to determine the centers contributing to the decomposition of the orbital. Then, an orbital is mixed with another orbitals if they share at least one nuclear center according to the given threshold, which we name below "threshold on orbital mixing" (TM).

We test several values of TM in the **VMC** wave function optimization of the PSB2, PSB3, and PSB4 and list the results in Table VI. We find that both ground- and excited-state energies are of course higher when we apply this threshold since we loose some degree of variationality in the optimization. On the other hand, the excitation energy remains unchanged and the computational saving is significant being as large as a factor of 6 in the number of orbital parameters to optimize for the largest PSB4. Therefore, this trick to cut the computational cost in the orbital optimization step is effective and allows one to treat both states on an equal footing.

TABLE VI. VMC total and excitation energies of the PSBn models computed with the Res-1 localized orbitals and different thresholds on the orbital mixing in the wave function optimization. The S0 B3LYP geometry is used.

Molecule	Thr. mixing (parms optimized)	E(S0) (a.u.)	E(S1) (a.u.)	ΔE (eV)
PSB2*	0.0 (579)	-30.2664(3)	-30.0458(3)	6.00(1)
	0.1 (190)	-30.2626(3)	-30.0416(3)	6.01(1)
	0.2 (170)	-30.2614(3)	-30.0408(3)	6.00(1)
PSB3†	0.00 (1213)	-42.8046(5)	-42.6441(5)	4.37(2)
	0.05 (309)	-42.7989(5)	-42.6382(5)	4.37(2)
	0.10 (290)	-42.7977(5)	-42.6372(5)	4.37(2)
	0.20 (270)	-42.7974(5)	-42.6359(5)	4.39(2)
	0.30 (257)	-42.7963(5)	-42.6357(5)	4.37(2)
PSB4‡	0.00 (2079)	-55.3447(5)	-55.2125(5)	3.60(2)
	0.10 (390)	-55.3359(5)	-55.2035(5)	3.60(2)
	0.20 (364)	-55.3348(5)	-55.2017(5)	3.62(2)
	0.30 (349)	-55.3338(5)	-55.2010(5)	3.61(2)

* All CAS(4,4) determinants are included.

† All singles, doubles, and triples in the CAS(6,6).

‡ CSFs with $|c_i|^2 > 0.011$ ($\sim$99% of CASSCF weight of both states)

III. COMPUTATIONAL DETAILS

The QMC calculations are performed with the CHAMP program [33] with scalar-relativistic energy-consistent Hartree-Fock pseudopotentials and the corresponding basis sets [34, 35]. In particular, we use the double (D), triple (T′) and quadrupole (Q′) basis sets, where the prime denotes that a double (D) basis is used for the hydrogen atoms, and the cc-pVDZ′ (D+) basis set which is a double basis set augmented with additional s and p functions on the heavy atoms [36]. To account for electron-electron and electron-nucleus correlations, we use a two-body Jastrow factor which is different for every atom types [37]. The Jastrow parameters, CI coefficients, and orbital coefficients are optimized with the linear method [38] in a state-averaged fashion [39] within VMC. **In the diffusion Monte Carlo (DMC) calculations, we treat the non-local pseudopotentials beyond the locality approximation [40] and use an imaginary time-step of 0.01 a.u. (for a time-step convergence study of the energies see the SI).**

To determine the initial inactive localized orbitals for the VMC trial wave function, several localization techniques [41–44] are possible, which unitarily transform the delocalized CASSCF orbitals into 1-or-2-centered localized orbitals. Here, we employ the Pipek-Mezey method [41] to localize the inactive and the virtual orbitals using the Molcas-7.8 [45] package. For the active space, we are interested in constructing localized orbitals that are mainly located on the atom/bond associated with a particular Lewis resonance structure. To this aim, we construct an initial guess of active orbitals with the desired structure, whose shape we find to be preserved in the

subsequent CASSCF calculation. For the Res-1 structure, the initial localized guess are obtained in a multi-configuration self-consistent-field calculation including the reference and a set of bonding-antibonding double excitations using the GAMESS(US) code [46, 47]. The initial localized active orbitals for the other resonance structures are prepared manually.

Upon optimization in VMC, we find that the active orbital might become delocalized and this undermines the construction of the multi-determinant expansion based on the concept of domains and excitation classes. We find that, to ensure the locality of active orbitals, it is sufficient to limit the mixing of the active orbitals among themselves: A bonding orbital is only mixed with its adjacent bonding orbitals and the antibonding orbitals that share at least one nucleus; an antibonding orbital is only mixed with a bonding orbital that shares one nucleus but not with other antibonding ones. This restricted orbital mixing is described in detail for PSBn (n = 2, 3, 4) in the Supporting Information (Tables S3, S10, and S21).

We perform excited state geometry optimizations of the PSB3 at the level of multi-state complete-active-space second-order perturbation theory (MS-CASPT2) [48–50] using the Molcas-7.8 package. We use the Cholesky decomposition of the two-electron integrals [51] with a threshold of 10^{-4} and always adopt the default 0.25 IPEA zero-order Hamiltonian [52]. We study the convergence of the optimal excited-state bond lengths using the Dunning correlation consistent cc-pVXZ and aug-cc-pVXZ basis sets [36, 53]. Finally, we optimize the ground-state geometry of the PSBn chromophores within DFT with the B3LYP functional [54–56] and the cc-pVDZ basis set using the Gaussian code [57] and the S1 planar bond-inverted CASSCF geometries with the cc-pVDZ basis and the Molcas-7.8 package.

IV. RESULTS

We test our novel form of Jastrow-Slater wave functions for excited states using the retinal protonated Schiff base model chromophores depicted in Figure 2. The smallest PSB2 model has two conjugated π bonds and by adding one and two more ethylenic groups, one obtains the PSB3 and PSB4 chromophores.

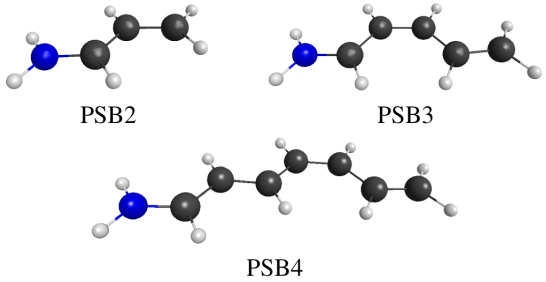

FIG. 2. Molecules studied in this work. Blue, black, and grey represent nitrogen, carbon, and hydrogen, respectively.

To assess the flexibility of the domain and multi-resonance concepts, we compute the VMC vertical excitation energies of the $\pi \rightarrow \pi^*$ state of the PSBn molecules at two in-plane geometries with different bond-length patterns and compare them with the reference values obtained using a complete (or nearly complete) expansion over the active orbitals (the configurations in the reference cover at least $\sim$99% of the CASSCF weights in the ground and excited states). The two test geometries are characterized by a positive and a negative value of the bond-length alternation (BLA) which we define as the difference between the averages of formal single and double C−C bonds, where "formal" refers to the ground-state geometry (or Res-1 Lewis structure). The two geometries are the ground-state B3LYP geometry and the bond-inverted S1 CASSCF geometry, respectively. To test the performance of our method in the relaxation of excited states, we also perform the out-of-plane excited-state geometry optimization of PSB3 at the VMC level. **Finally, we compute the DMC total and excitation energies for single and multi-resonance local wave functions at the ground-state geometry.**

A. PSB2

The minimal active space to describe the $\pi \rightarrow \pi^*$ excited state in PSB2 is a CAS(4,4) expansion where we correlate 4 electrons in 4 π orbitals. The molecule has two resonance structures with corresponding localized active π orbitals shown in Figure 3.

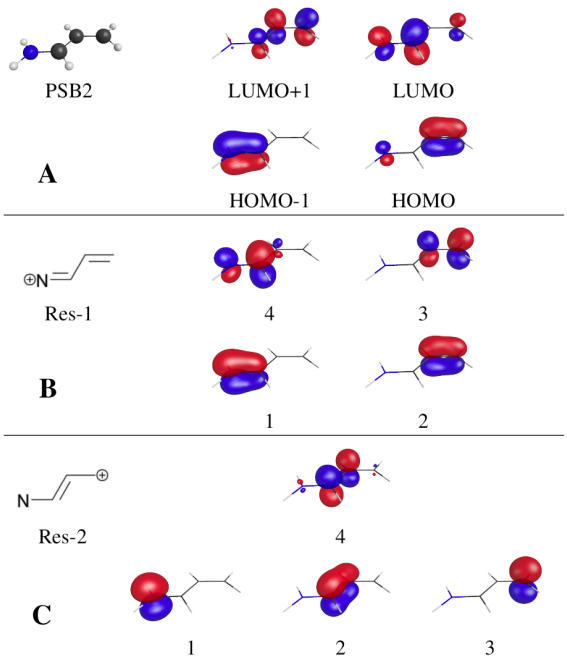

FIG. 3. PSB2: (A) Active delocalized π orbitals obtained at the CASSCF(4,4) level, and (B,C) two unitary transformed sets of localized orbitals corresponding to the two Lewis resonance structures.

Before addressing the performance of the wave functions proposed here for PSB2, we investigate the effect of using dif-

ferent active spaces, number of determinants, and basis sets on the vertical excitation energy at the VMC level. In these tests, the determinantal expansion is expressed on the delocalized natural orbitals and all parameters of the wave function are optimized. In particular, all (inactive and active) orbitals are mixed with the active and virtual ones according to the symmetry. For the larger active spaces, the expansion is truncated according to a threshold on the CI coefficients on both states, and the union of the surviving configurations is retained in the Jastrow-Slater wave functions. The results are collected in Table VII.

TABLE VII. PSB2: VMC Energies computed with different basis sets and active spaces expressed on the weighted-averaged natural orbitals at the S0 B3LYP geometry.

Active Space	Thr. (N det)	Basis	E(S0) (a.u.)	E(S1) (a.u.)	ΔE (eV)
CAS(4,4)	0.00 (36)	D	-30.2661(3)	-30.0460(3)	5.99(1)
CAS(4,6)	0.02 (58)	D	-30.2677(3)	-30.0471(3)	6.00(1)
CAS(4,6)	0.01 (99)	D	-30.2677(3)	-30.0478(3)	5.98(1)
CAS(4,8)	0.02 (83)	D	-30.2677(3)	-30.0471(3)	6.00(1)
CAS(4,8)	0.01 (125)	D	-30.2678(3)	-30.0479(3)	5.98(1)
CAS(4,4)	0.00 (36)	D+	-30.2673(3)	-30.0501(3)	5.91(1)
CAS(4,4)	0.00 (36)	T′	-30.2782(3)	-30.0602(3)	5.93(1)
CAS(4,4)	0.00 (36)	Q′	-30.2793(3)	-30.0621(3)	5.91(1)

We find that enlarging the active space beyond the minimal one with the inclusion of additional π orbitals results in the decrease of the energies of both states but that the excitation energy remains compatible within the statistical error. The choice of basis set has a larger impact on the the excitation energy, which is however practically converged with the D+ basis set **at both the VMC and DMC level (see Table S27)**. For the purpose of assessing our excited-state method, we select the CAS(2n,2n) active space and D basis set for the PSBn molecules as compromise between accuracy and computational cost, keeping in mind that, if one is interested in the best excitation energies of PSBn, one should use a larger basis set. **We also note that the use of a small CAS(2,2) expansion leads to errors in the excitation energies which grow with system size (see Table S24).**

We now begin the construction of the local wave functions, whose performance is assessed against a VMC calculation that includes all (36) determinants of the CAS(4,4) expansion. With this active space, the Res-1 localized orbitals consist of 2 bonding and 2 antibonding orbitals and the dominant doubly-occupied configurations (2200) is the reference configuration. In the CASSCF calculation, there are 3 important singles, which result in the domains:

a) $\{1:4\}$
b) $\{2:3,4\}$

As in the case of PSB3, the charge transfer character of the excited state is evident from the domains as the most important single ($2 \rightarrow 4$) results in a net charge transfer from the C-terminus to the N-terminus (see Table S1). For the Res-2 structure, we can place 4 electrons in 3 bonding and 1 antibonding orbitals and, if the three possible doubly-occupied configurations, retain 2 references for establishing the domains, namely, 2200 and 2020. The remaining doubly-occupied configuration (0220) is unimportant since its weight is almost 0% in both states. The domains of the 2200 reference are

1a) $\{1:3,4\}$
1b) $\{2:3\}$

while, for the 2020 reference, we have

2a) $\{1:2\}$

The excitation classes are constructed and ordered in the same way as for PSB3 (see Method Section) and the resulting configurational weights are listed in Table VIII, for the Res-1 structure at the ground-state geometry and for Res-2 at the bond-inverted geometry, respectively.

TABLE VIII. PSB2: CASSCF weight percentage of the excitation classes of the Res-1 and the Res-2 structure at the in-plane S0 B3LYP and the bond-inverted S1 CASSCF geometry, respectively.

	Res-1			Res-2		
	Det	Weight (%)		Det	Weight (%)	
	(N)	S0	S1	(N)	S0	S1
X0	1	93.60	0.05	2	18.13	16.40
X1	6	0.63	91.67	8	75.37	74.78
X3	2	4.84	4.75	1	0.25	0.24
X4	1	0.24	2.24	1	0.01	0.08
X5	6	0.22	0.25	6	3.12	4.87
X6	2	0.00	0.06			
X7	2	0.21	0.00	2	0.14	0.41
X8	4	0.00	0.23	2	0.41	2.34
Total	**24**	**99.74**	**99.25**	**22**	**97.41**	**99.12**

Here, we want to understand the minimum set of ingredients in the local wave functions needed to yield the reference energies. Therefore, we include systematically the excitation classes of one and two resonance structures in the Jastrow-Slater trial wave functions of PSB2 and fully reoptimize each trial wave function in VMC. The resulting ground- and excited-state energies computed at the ground-state and bond-inverted geometries are reported in Table IX. At the equilibrium geometry, if we use a single Res-1 structure, we find that the excitation energy is already converged with the inclusion of the X0–X4 excitation classes (10 determinants). On the other hand, the ground- and excited-state energies display a slower convergence, which is is only achieved when all X0–X8 transitions (24 determinants) are included.

If we employ a multi-resonance Jastrow-Slater wave function and account for both the Res-1 and Res-2 resonances in the multi-determinantal wave function, the energies of both states are already in agreement with the reference values when we include the sole X0-X3 classes for each resonance. Consequently, we obtain a somewhat more compact (20 determinants) wave function for PSB2 when using two instead of a

single resonance structure. If we perform a similar analysis on the bond-inverted geometry of PSB2, we obtain an equivalently good performance of the multi-resonance wave function expressed on the X0–X3 excitations of both resonance structures.

We note that, in the orbital optimization step, the active orbitals become occasionally delocalized and that the loss in locality is especially pronounced when moving to larger systems. Therefore, all results for PSB2 in Table IX (as well as below for PSB3 and PSB4) are obtained with the restriction on the mixing among the active orbitals described in the Computational Details. This restriction is found to generally preserve locality but leads to an increase in the energies (as documented in Table S4) and is in part responsible for their slower convergence with the excitation classes. The effect of this restriction becomes however negligible once we include the X0-X8 excitation classes or multiple resonances in combination with fewer classes. In Table IX, we further test the effect of limiting the occupied-virtual orbital mixing in the orbital optimization of the multi-resonance wave function by applying a threshold TM $= 0.2$. We find that, at both geometries, the energies of the S0 and S1 states raise by about 4–5 mHartree but that the excitation energies remain compatible with the reference values.

TABLE IX. PSB2: VMC total and excitation energies computed with an increasing number of excitation classes of one or two resonance structures at the S0 B3LYP (BLA > 0) and S1 CASSCF (BLA < 0) geometries.

Resonance	Determinant (N)	S0 (a.u.)	S1 (a.u.)	ΔE (eV)
BLA > 0 geometry				
1	X0–X1 (7)	–*	–*	–*
1	X0–X3 (9)	-30.2638(3)	-30.0403(3)	6.08(1)
1	X0–X4 (10)	-30.2649(3)	-30.0437(3)	6.02(1)
1	X0–X5 (16)	-30.2651(3)	-30.0444(3)	6.01(1)
1	X0–X6 (18)	-30.2651(3)	-30.0437(3)	6.02(1)
1	X0–X7 (20)	-30.2652(3)	-30.0442(3)	6.01(1)
1	X0–X8 (24)	-30.2656(3)	-30.0449(3)	6.01(1)
1,2	X0–X1 (17)	–*	–*	–*
1,2	X0–X3 (20)	-30.2670(3)	-30.0464(3)	6.00(1)
1,2†	X0–X3 (20)	-30.2616(3)	-30.0412(3)	6.00(1)
1	All (36)	-30.2664(3)	-30.0458(3)	6.00(1)
BLA < 0 geometry				
1,2	X0–X3 (20)	-30.2176(3)	-30.0512(3)	4.53(1)
1,2†	X0–X3 (20)	-30.2128(3)	-30.0455(3)	4.55(1)
1	All (36)	-30.2175(3)	-30.0513(3)	4.52(1)

* The run results in delocalized optimized active orbitals.

† TM $= 0.2$ on the occupied-virtual orbital mixing.

B. PSB3

The construction of the excitation classes of the Res-1 and Res-2 structures of PSB3 is explained in detail in the Method Section whereas the construction for the Res-3 structure is described in the SI. Having all excitation classes built, we can progressively add them in the wave function as shown in Table X. The reference energies are computed as an expansion over all singles, doubles, and triples excitations expressed in terms of the Res-1 orbitals, whose total weight at the SA-CASSCF level is more than 99% for both states. Note that we restrict the active orbital mixing in the orbital optimization as for PSB2 to guarantee their locality upon optimization.

TABLE X. PSB3: VMC total and excitation energies computed with an increasing number of excitation classes of one, two, and three resonance structures at the S0 B3LYP (BLA > 0) and S1 CASSCF (BLA < 0) geometries.

Resonance	Determinant	S0 (a.u.)	S1 (a.u.)	ΔE (eV)
BLA > 0 geometry				
1	X0–X2 (13)	-42.7865(5)	-42.6150(5)	4.67(2)
1	X0–X3 (16)	-42.7980(5)	-42.6262(5)	4.67(2)
1	X0–X4 (18)	-42.8002(5)	-42.6292(5)	4.65(2)
1	X0–X5 (36)	-42.7989(5)	-42.6359(5)	4.44(2)
1	X0–X6 (40)	-42.8012(5)	-42.6369(5)	4.47(2)
1	X0–X7 (48)	-42.8017(5)	-42.6382(5)	4.45(2)
1	X0–X8 (56)	-42.8015(5)	-42.6392(5)	4.42(2)
1,2	X0–X3 (41)	-42.8029(5)	-42.6396(5)	4.44(2)
1,2	X0–X4 (43)	-42.8032(5)	-42.6406(5)	4.42(2)
1,2	X0–X5 (79)	-42.8041(5)	-42.6412(5)	4.43(2)
1,2	X0–X6 (85)	-42.8037(8)	-42.6403(8)	4.45(3)
1,2	X0–X7 (93)	-42.8041(5)	-42.6410(5)	4.44(2)
1,2	X0–X8 (119)	-42.8039(5)	-42.6396(5)	4.47(2)
1,2,3	X0–X3 (66)	-42.8045(5)	-42.6431(5)	4.39(2)
1,2,3 †	X0–X3 (66)	-42.7973(5)	-42.6352(5)	4.41(2)
Reference ‡		-42.8046(5)	-42.6441(5)	4.37(2)
BLA < 0 geometry				
1,2,3	X0–X3 (66)	-42.7823(5)	-42.6470(5)	3.68(2)
1,2,3 †	X0–X3 (66)	-42.7740(5)	-42.6385(5)	3.69(2)
Reference ‡		-42.7823(5)	-42.6468(5)	3.69(2)

† TM $= 0.2$ on the occupied-virtual orbital mixing.

‡ All singles, doubles, and triples with the Res-1 orbitals (282 determinants)

Differently from the case of the PSB2, the convergence of the excitation energy and the total energies of both states is not achieved with by including the X0–X8 excitation classes of one (Res-1) or two (Res-1 and Res-2) resonance structures. While the ground-state energy is converged with a wave function expressed on the X0–X5 transitions of the Res-1 and Res-2 structures (79 determinants), the excited-state energy needs more configurations to reach its reference value. We stress that the lack of convergence is here not due to the restriction

on the mixing among the active orbitals in the wave function optimization (see Table S11). Therefore, one needs to construct and include additional excitation classes (X9, X10, etc.) if one keeps the expansion over one or two resonance structures.

If we include also the remaining resonance structure (Res-3) and add the corresponding excitation classes, we obtain that the convergence of the energy of both states and, consequently, of the excitation energy is reached by just including the X0–X3 excitation classes of all three resonance structures in the expansion. This wave function is compact and only contains 66 determinants. The same multi-resonance expansion is employed for the bond-inverted geometry and is found to describe equally well both states and the excitation energy, which are in agreement with the reference values. We can further reduce the computational cost by applying TM $= 0.2$ in the optimization of the wave function which leads to an increase of the energies of both states by about 8–9 mHartree but to a compatible excitation energy.

C. PSB4

The largest retinal model investigated in this work is PSB4 which has four dominant Lewis resonance structures as depicted in Figure 4. At the ground-state equilibrium geometry, the wave function of the $\pi \rightarrow \pi^*$ excited state is dominated by the Res-1 structure while the other resonances become more important in the relaxation process. The analysis of the domains, excitation classes, and weights in the localized CASSCF wave functions for the four resonance structures is included in the SI.

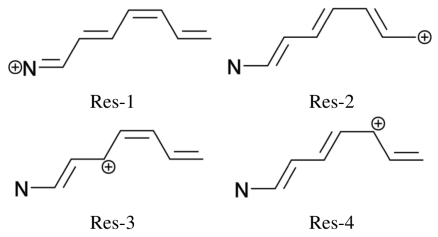

FIG. 4. PSB4: Lewis structures. The corresponding CAS(8,8) localized active orbitals are reported in Figure S3.

Also for PSB4, we test the performance of the multi-resonance wave function that includes the X0–X3 excitation classes of all possible resonance structures and report the results in Table XI. To compute the reference energies, we construct Jastrow-Slater wave functions with determinantal expansions over delocalized natural orbitals, which recover at least 99% of the CASSCF weights of both states. At both the equilibrium ground-state and the bond-inverted in-plane geometry, the ground- and excited-state energies and the excitation energy of the multi-resonance wave functions are in very good agreement with the reference values. The resulting wave function is very compact with a number of determinants (159) which is lower by a factor of 2–3 at the two geometries than the one used to compute the reference energies. Further reduction of computational cost can be obtained by applying a TM $= 0.2$ in the orbital optimization step to limit the occupied-virtual orbital mixing (the number of parameter to optimize is reduced by almost a factor of 6 – see Table VI). As in the case of PSB2 and PSB3, the resulting energy gap remains compatible with the reference value.

TABLE XI. PSB4: VMC total and excitation energies computed with a wave function including all resonance structures at the S0 B3LYP (BLA > 0) and S1 CASSCF (BLA < 0) geometries.

Resonance	Determinant	S0 (a.u.)	S1 (a.u.)	ΔE (eV)
BLA > 0 geometry				
1,2,3,4	X0–X3 (159)	-55.3454(5)	-55.2128(5)	3.61(2)
1,2,3,4*	X0–X3 (159)	-55.3346(5)	-55.2011(5)	3.63(2)
Reference†	(433)	-55.3441(5)	-55.2123(5)	3.59(2)
BLA < 0 geometry				
1,2,3,4	X0–X3 (159)	-55.3237(5)	-55.2149(5)	2.96(2)
1,2,3,4*	X0–X3 (159)	-55.3129(5)	-55.2037(5)	2.97(2)
Reference†	(485)	-55.3238(5)	-55.2160(5)	2.93(2)

$*$ TM $= 0.2$ on the occupied-virtual orbital mixing

† $\sim$99% of CASSCF weights on delocalized natural orbitals.

D. Geometry Optimization

The wave function expanded on the X0–X3 excitation classes of all possible resonance structures is a compact and accurate wave function for the computation of the vertical excitation energies of PSBn (n = 2,3,4) at two different in-plane geometries. We now test its ability to describe the excited-state relaxation by performing the out-of-plane geometry optimization of one retinal model chromophore, namely, the PSB3. To reduce the computational cost, we apply TM $= 0.2$ in the orbital optimization and compare the resulting optimized geometries against the ones obtained from a fully optimized Jastrow-Slater wave function whose determinantal expansion over delocalized natural orbitals is truncated to recover 99% of the total CASSCF weight of both states. We also compare the VMC excited-state geometries to the optimal CASPT2 ones.

The relevant optimized excited-state geometrical parameters are shown in Table XII. The atoms are numbered and the covalent bonds ordered as N_1=C_1–C_2=C_3–C_4=C_5. We find that the optimized geometrical parameters obtained with the local multi-resonance wave function differ by less than 3 mÅ and 1^o from the VMC reference values computed with the same D basis set. This demonstrates the good performance of our localized representation of the wave function also in the optimization of the excited-state geometry. Finally, to compare the VMC and MS-CASPT2 geometries, we employ the triple- and quadruple-zeta (double-zeta for hydrogens) basis sets, respectively, since VMC benefits from a somewhat faster basis-set convergence of the structural parameters (see Table

S15) and observe an excellent agreement between the equilibrium structures obtained with the two methods with differences smaller than 7 mÅ and 2^o.

TABLE XII. PSB3: VMC out-of-plane optimized geometries.

Method	VMC			CASPT2(6,6)
	Reference*	Local†	Local†	
Basis set	D	D	T′	cc-pVQZ′
N_1=C_1	1.3800(2)	1.3801(7)	1.3738(4)	1.3740
C_1–C_2	1.4674(1)	1.4666(14)	1.4619(7)	1.4598
C_2=C_3	1.3981(2)	1.4009(7)	1.3934(3)	1.3951
C_3–C_4	1.4003(2)	1.4007(6)	1.3948(5)	1.4015
C_4=C_5	1.3823(1)	1.3811(9)	1.3720(4)	1.3787
BLA	0.0436(4)	0.0459(8)	0.0474(4)	0.0438
$\theta^{\ddagger}$	4.76(5)	4.48(5)	2.63(4)	1.8
$\gamma^{\#}$	72.20(4)	72.4(1)	73.56(4)	75.4

* ∼99% of CASSCF weights on delocalized natural orbitals.

† X0–X3 classes of all resonances and TM $= 0.2$

‡ θ =Dih(C_1–C_2=C_3–C_4).

γ =180^o−Dih(C_2=C_3–C_4=C_5).

TABLE XIII. PSBn: DMC total and excitation energies computed with single and multi resonance local wave functions at the in-plane S0 B3LYP equilibrium geometry.

Resonance	Determinant	S0 (a.u.)	S1 (a.u.)	ΔE (eV)
PSB2				
1	X0–X3 (9)	-30.3347(3)	-30.1169(3)	5.93(1)
1,2	X0–X3 (20)	-30.3357(3)	-30.1206(3)	5.85(1)
Reference*	(36)	-30.3360(3)	-30.1208(3)	5.86(1)
PSB3				
1	X0–X3 (16)	-42.9010(5)	-42.7377(5)	4.44(2)
1,2	X0–X3 (41)	-42.9042(4)	-42.7454(5)	4.32(2)
1,2,3	X0–X3 (66)	-42.9037(4)	-42.7470(4)	4.26(2)
Reference†	(282)	-42.9042(4)	-42.7470(4)	4.28(2)
PSB4				
1,2,3,4	X0–X3 (159)	-55.4735(4)	-55.3451(4)	3.49(2)
Reference‡	(433)	-55.4739(5)	-55.3466(5)	3.46(2)

* All CAS(4,4) determinants are included.

† All singles, doubles, and triples with the Res-1 orbitals

‡ ∼99% of CASSCF weights on delocalized natural orbitals.

E. DMC calculations

For the ground-state geometries (BLA > 0) of all models, we compute the DMC ground- and excited-state energies and the corresponding excitation energies using as trial wave functions the fully optimized single and multi-resonance local wave functions presented above.

As shown in Table XIII, we find that the DMC results follow the behavior of the VMC ones (see Tables IX, X, and XI). In particular, both total and excitation energies are in very good agreement with the reference values if the X0-X3 classes of all dominant Lewis resonance structures are included in the determinantal component of the trial wave function. This is however not the case if one employs fewer resonance structures and the same small set of X0-X3 excitations.

V. CONCLUSIONS

We have developed a novel class of compact multideterminantal Jastrow-Slater wave functions based on localized orbitals that can be progressively extended to higher quality and accurately treat on an equal footing the ground and the excited states in QMC calculations. Since excited states may in general be characterized by charge transfer, the orbitals to correlate in the determinantal expansion cannot be selected based on their spacial vicinity as we had done in our previous work on ground states. To establish a criterion to account for the most important transitions in the excited state, we borrowed the concept of orbital domains from local coupled-cluster methods and applied it to the local orbitals in the active space. For each doubly-occupied reference configuration, an occupied orbital and the set of orbitals coupled to it by large single-electron transitions are grouped in an orbital domain, the dominant domains are identified, and the subsequent excitations constructed within and from the union of the surviving domains. Bonding-antibonding double excitations are always included being the most important configurations after the reference(s) in the ground state. The resulting excitations are collected into classes that are ordered in importance and can then be systematically included in the determinantal component of the Jastrow-Slater wave function.

To further enhance the description of the states of interest (in particular, the excited states), we have also accounted for the presence of multiple Lewis resonance structures in the molecule. For a given representation of the delocalized orbitals in the active space, multiple set of equivalent local orbitals can be built corresponding to the different Lewis structures. These sets are no longer equivalent if we depart from the complete expansion, as we do when using the concept of domains, and each set may offer a better description of the different states in different parts of the potential energy surface. We first verified that our scheme of constructing and classifying the orbital domains and excitation classes is transferable to all sets of local orbitals (resonance structure) and then constructed multiple-resonance Jastrow-Slater wave functions as linear combinations of classes of excitations built from the domains of all the different Lewis structures.

The method was demonstrated at the variational **and diffusion** Monte Carlo level on the vertical excitation energies of the $\pi \rightarrow \pi^*$ state of the retinal protonated Schiff base model chromophores, PSBn (n = 2,3,4), which represent a challenging system due to the strong intra-molecular charge-transfer character of the transition. To test the flexibility of our wave functions, we performed the calculations at two geometries

with very different bond-length patterns and therefore better described in terms of different dominant Lewis resonance structures. We found that, while the use of one resonance structure and a small expansion is sufficient in the smallest PSB2 model, the convergence of the excited-state **VMC energy with the** number of excitation classes becomes increasingly slower for the larger models. On the other hand, if one uses a multi-resonance wave function expanded over all possible Lewis structures, few excitation classes (i.e. the reference(s), important singles, and bonding-antibonding doubles) are needed to accurately describe the ground and excited states of the PSBn, yielding total VMC energies in agreement with the reference values **obtained with large determinantal expansions**. **The same behavior is observed at the DMC level.** Importantly, the same set of excitation classes can be employed to describe both states successfully at the two different geometries considered, whereas one would in general obtain different determinantal expansions when truncating the wave function expressed on delocalized orbitals as often done in QMC calculations. We also employed this compact multi-resonance wave function to determine the relaxed out-of-plane excited-state geometry of PSB3 and obtained geometrical parameters in agreement with the VMC reference calculation. Finally, we showed the additional benefit of the use of local orbitals in the orbital optimization step, whose cost can be significantly reduced by limiting the mixing of the occupied and virtual orbitals based on spacial consideration without sacrificing the quality of the excitation energy.

In summary, we have developed a successful procedure to construct multi-resonance local Jastrow-Slater wave functions that give a balanced description of the ground and the excited states also in systems where distant orbitals are strongly correlated. The resulting expansion is compact and transferable to different geometries without adjustments. For the largest PSB4 model considered here, the size of the domains is still growing but the expansion is already reduced by a factor of 2–3 as compared to the minimum number of determinants in the delocalized-orbital basis, which is needed to achieve converged total energies for both states. As the system grows further, the spatially remote orbitals will become weakly correlated and the size of the domains saturate (see Tables S28 and S29 for PSB5 and PSB6, respectively), leading to further significant gains over a calculations using delocalized orbitals. In conclusion, the compactness and accuracy of the expansion, its transferability to different geometries, and the reduction of the orbital optimization cost are very promising features of our novel multi-resonance local wave functions, offering a robust and affordable route to excited-state calculations of large molecular systems in QMC.

SUPPORTING INFORMATION

The Supporting Information is available free of charge on the ACS Publications website.

Analysis of orbital domains; effect of orbital optimization on the VMC energies of multi-resonance local wave functions; convergence study of the VMC total energies obtained using a truncated expansion on delocalized natural orbitals (with and without orbital optimization); **VMC energies of small CAS(2,2) wave functions; imaginary time-step and basis-set convergence of the DMC total and excitation energies of PSB2;** basis-set convergence of the out-of-plane excited-state MS-CASPT2 optimal geometry of PSB3; XYZ coordinates of all models at the various geometries used to analyze the wave functions.

AUTHOR INFORMATION

The corresponding author is Claudia Filippi, email: c.filippi@utwente.nl

ACKNOWLEDGEMENTS

We thank NWO for the use of the SARA supercomputer facilities.

[1] P. Pulay, Chem. Phys. Lett. **100**, 151 (1983).
[2] C. Hampel and H.-J. Werner, J. Chem. Phys. **104**, 6286 (1996).
[3] M. Schütz and H.-J. Werner, J. Chem. Phys. **114**, 661 (2001).
[4] B. Bories, D. Maynau, and M.-L. Bonnet, J. Comput. Chem. **28**, 632 (2007).
[5] F. Neese, F. Wennmohs, and A. Hansen, J. Chem. Phys. **130**, 114108 (2009).
[6] F. Neese, A. Hansen, and D. G. Liakos, J. Chem. Phys. **131**, 064103 (2009).
[7] S. Saebo and P. Pulay, Annu. Rev. Phys. Chem. **44**, 213 (1993).
[8] P. Reinhardt, H. Zhang, J. Ma, and J.-P. Malrieu, J. Chem. Phys. **129**, 164106 (2008).
[9] H. Zhang, J.-P. Malrieu, P. Reinhardt, and J. Ma, J. Chem. Phys. **132**, 034108 (2010).
[10] C. Riplinger and F. Neese, J. Chem. Phys. **138**, 034106 (2013).
[11] C. Riplinger, B. Sandhoefer, A. Hansen, and F. Neese, J. Chem. Phys. **139**, 134101 (2013).
[12] P. E. Maslen and M. Head-Gordon, Chemi. Phys. Lett. **283**, 102 (1998).
[13] P. E. Maslen and M. Head-Gordon, J. Chem. Phys. **109**, 7093 (1998).
[14] G. E. Scuseria and P. Y. Ayala, J. Chem. Phys. **111**, 8330 (1999).
[15] M. Schütz, G. Hetzer, and H.-J. Werner, J. Chem. Phys. **111**, 5691 (1999).
[16] N. B. Amor, F. Bessac, S. Hoyau, and D. Maynau, J. Chem. Phys. **135**, 014101 (2011).
[17] C. Chang, C. J. Calzado, N. B. Amor, J. S. Marin, and D. Maynau, J. Chem. Phys. **137**, 104102 (2012).
[18] D. Walter, A. Venkatnathan, and E. A. Carter, J. Chem. Phys. **118**, 8127 (2003).

[19] T. S. Chwee, A. B. Szilva, R. Lindh, and E. A. Carter, J. Chem. Phys. **128**, 224106 (2008).

[20] D. B. Krisiloff and E. A. Carter, Phys. Chem. Chem. Phys. **14**, 7710 (2012).

[21] O. Demel, J. Pittner, and F. Neese, J. Chem. Theory Comput. **11**, 3104 (2015).

[22] T. Korona and H.-J. Werner, J. Chem. Phys. **118**, 3006 (2003).

[23] T. D. Crawford and R. A. King, Chem. Phys. Lett. **366**, 611 (2002).

[24] D. Kats, T. Korona, and M. Schütz, J. Chem. Phys. **125**, 104106 (2006).

[25] B. Helmich and C. Hättig, J. Chem. Phys. **135**, 214106 (2011).

[26] B. Helmich and C. Hättig, J. Chem. Phys. **139**, 084114 (2013).

[27] T. S. Chwee and E. A. Carter, J. Chem. Theory Comput. **7**, 103 (2010).

[28] F. Fracchia, C. Filippi, and C. Amovilli, J. Chem. Theory Comput. **8**, 1943 (2012).

[29] F. Fracchia, C. Filippi, and C. Amovilli, J. Chem. Theory Comput. **9**, 3453 (2013).

[30] F. Fracchia, C. Filippi, and C. Amovilli, J. Comput. Chem. **35**, 30 (2014).

[31] A. G. Anderson and W. A. Goddard III, J. Chem. Phys. **132**, 164110 (2010).

[32] B. Braïda, J. Toulouse, M. Caffarel, and C. Umrigar, J. Chem. Phys. **134**, 084108 (2011).

[33] CHAMP is a quantum Monte Carlo program package written by Umrigar, C. J.; Filippi, C. and collaborators.

[34] M. Burkatzki, C. Filippi, and M. Dolg, J. Chem. Phys. **126**, 234105 (2007).

[35] For the hydrogen atom, we use a more accurate BFD pseudopotential and basis set. M. Dolg and C. Filippi, private communication.

[36] R. A. Kendall, T. H. Dunning Jr, and R. J. Harrison, J. Chem. Phys. **96**, 6796 (1992).

[37] C. Filippi and C. J. Umrigar, J. Chem. Phys. **105**, 213 (1996).

[38] C. J. Umrigar, J. Toulouse, C. Filippi, S. Sorella, and R. G. Hennig, Phys. Rev. Lett. **98**, 110201 (2007).

[39] C. Filippi, M. Zaccheddu, and F. Buda, J. Chem. Theory Comput. **5**, 2074 (2009).

[40] M. Casula, Phys. Rev. B **74**, 161102 (2006).

[41] J. Pipek and P. G. Mezey, J. Chem. Phys. **90**, 4916 (1989).

[42] S. F. Boys, Rev. Mod. Phys. **32**, 296 (1960).

[43] J. M. Foster and S. F. Boys, Rev. Mod. Phys. **32**, 300 (1960).

[44] C. Edmiston and K. Ruedenberg, Rev. Mod. Phys. **35**, 457 (1963).

[45] F. Aquilante, L. De Vico, N. Ferré, G. Ghigo, P.-å. Malmqvist, P. Neogrády, T. B. Pedersen, M. Pitoňák, M. Reiher, B. O. Roos, L. Serrano-Andrés, M. Urban, V. Veryazov, and R. Lindh, J. Comput. Chem. **31**, 224 (2010).

[46] M. W. Schmidt, K. K. Baldridge, J. A. Boatz, S. T. Elbert, M. S. Gordon, J. H. Jensen, S. Koseki, N. Matsunaga, K. A. Nguyen, S. Su, T. L. Windus, M. Dupuis, and J. A. Montgomery, J. Comput. Chem. **14**, 1347 (1993).

[47] M. S. Gordon and M. W. Schmidt, in *Theory and Applications of Computational Chemistry: the first forty years*, edited by C. Dykstra, G. Frenking, K. Kim, and G. Scuseria (Elsevier, Amsterdam, 2011) Chap. 41, pp. 1167–1190.

[48] K. Andersson, P.-Å. Malmqvist, B. O. Roos, A. J. Sadlej, and K. Wolinski, J. Phys. Chem. **94**, 5483 (1990).

[49] K. Andersson, P.-Å. Malmqvist, and B. O. Roos, J. Chem. Phys. **96**, 1218 (1992).

[50] J. Finley, P.-Å. Malmqvist, B. O. Roos, and L. Serrano-Andrés, Chem. Phys. Lett. **288**, 299 (1998).

[51] F. Aquilante, P.-Å. Malmqvist, T. B. Pedersen, A. Ghosh, and B. O. Roos, J. Chem. Theory Comput. **4**, 694 (2008).

[52] G. Ghigo, B. O. Roos, and P.-Å. Malmqvist, Chem. Phys. Lett. **396**, 142 (2004).

[53] T. H. Dunning Jr, J. Chem. Phys. **90**, 1007 (1989).

[54] A. D. Becke, Phys. Rev. A. **38**, 3098 (1988).

[55] C. Lee, W. Yang, and R. G. Parr, Phys. Rev. B. **37**, 785 (1988).

[56] A. D. Becke, J. Chem. Phys. **98**, 5648 (1993).

[57] M. J. Frisch, G. W. Trucks, H. B. Schlegel, G. E. Scuseria, M. A. Robb, J. R. Cheeseman, G. Scalmani, V. Barone, B. Mennucci, G. A. Petersson, H. Nakatsuji, M. Caricato, X. Li, H. P. Hratchian, A. F. Izmaylov, J. Bloino, G. Zheng, J. L. Sonnenberg, M. Hada, M. Ehara, K. Toyota, R. Fukuda, J. Hasegawa, M. Ishida, T. Nakajima, Y. Honda, O. Kitao, H. Nakai, T. Vreven, J. A. Montgomery, Jr., J. E. Peralta, F. Ogliaro, M. Bearpark, J. J. Heyd, E. Brothers, K. N. Kudin, V. N. Staroverov, R. Kobayashi, J. Normand, K. Raghavachari, A. Rendell, J. C. Burant, S. S. Iyengar, J. Tomasi, M. Cossi, N. Rega, J. M. Millam, M. Klene, J. E. Knox, J. B. Cross, V. Bakken, C. Adamo, J. Jaramillo, R. Gomperts, R. E. Stratmann, O. Yazyev, A. J. Austin, R. Cammi, C. Pomelli, J. W. Ochterski, R. L. Martin, K. Morokuma, V. G. Zakrzewski, G. A. Voth, P. Salvador, J. J. Dannenberg, S. Dapprich, A. D. Daniels, Ö. Farkas, J. B. Foresman, J. V. Ortiz, J. Cioslowski, and D. J. Fox, "Gaussian 09 Revision D.01," Gaussian Inc. Wallingford CT 2009.